INTERNATIONAL JOURNAL OF COMPUTERS COMMUNICATIONS & CONTROL
Online ISSN 1841-9844, ISSN-L 1841-9836, Volume: 19, Issue: 5, Month: October, Year: 2024
Article Number: 6620, https://doi.org/10.15837/ijccc.2024.5.6620

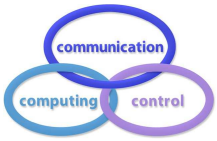

CCC Publications

Improved Sliding Mode Model Reference Adaptive System Observer

Gang Li

Gang Li
School of Electronic and Information Engineering
Sichuan Geely University,CHINA
123 Shipan Street, Jianyang City, Chengdu, Sichuan 641423,CHINA
ligangdzxxgc@guc.edu.cn

Abstract

In order to improve the accuracy and stability of sensorless control system of permanent magnet synchronous motor, considering the influence of external load torque on system performance, the symbol function of the sliding mode control system of the vehicle permanent magnet synchronous motor is prone to severe buffeting and the robustness of the traditional PI control is very insufficient.. In this paper, a method of combining Non-singular Fast Terminal Sliding Mode (NFTSM) and Model Reference Adaptive System (MRAS) is proposed. A Non-singular Fast Terminal Sliding Mode Controller (NFTSMC) is designed. A control strategy combining NFTSMC and Model Reference Adaptive System Observer (MRASO) (NFTSMC-MRASO) converts the observed torque value into torque current feedforward compensation to the current loop input. The method can convert the observed torque value into torque current feedforward compensation to the input end of the current loop, avoid large sliding mode gain, and overcome the system buffeting problem when the external disturbance is suddenly added. At the same time, the system robustness is improved under the premise of suppressing chattering.

Keywords: Permanent magnet synchronous motor, Buffeting; Robustness, Non-singular fast terminal sliding mode, Model reference adaptive system.

1 Introduction

In recent years, power electronics technology has developed rapidly. Permanent Magnet Synchronous Motor (PMSM) has the advantages of small size [1, 2, 3], light weight, high power density and large starting torque, and has been widely used in automobile, aerospace, robot and other fields.The symbol function of vehicle PMSM sliding mode control system is prone to serious chattering and the robustness of traditional PI control is very insufficient. Considering the influence of external load torque on system performance, a more suitable control method needs to be found in order to improve the accuracy and stability of sensorless control system of permanent magnet synchronous motor.

PMSM vector system in order to obtain high-performance dynamic and static operation quality [4, 5, 6], it is necessary to obtain accurate speed and position information through mechanical sensors [7], but PMSM usually works in harsh environments, and mechanical sensors are prone to environmental failure, thereby reducing the reliability of the system.As a variable structure nonlinear control

method, sliding mode control [8, 9, 10, 11, 12] has the advantages of fast response and strong robustness compared with traditional PI control, and is not sensitive to internal parameters and external disturbances, so it is widely used in PMSM speed regulation system. But one of the main disadvantages of sliding mode control is that chattering occurs when the system state variable moves near the sliding mode surface. To solve the buffeting problem has become a hot research issue in sliding mode control.The appearance of sensorless control technology [13, 14] has solved the above problems. Experts and scholars have carried out a lot of research on sensorless control technology. At present, sensorless control technology is mainly divided into two categories: one is high frequency signal injection method [15, 16], which is only applicable to zero speed and low speed; The other is observer method [17], which mainly includes sliding mode observer [18], extended Kalman filter [19] and model reference adaptive system observer (MRASO) [20]. Among them, MRASO is widely used because of its simple structure and small calculation amount, but its internal proportional integration is sensitive to internal and external disturbance parameters of the system, and there is a problem of insufficient robustness. For this reason, outstanding achievements have been made in the process of studying the model reference adaptive system observer in the world. A typical MRASO based on fuzzy PI improves the dynamic performance of the system by adjusting the coefficient of PI in real time through fuzzy rules [21]. However, the introduction of fuzzy algorithm undoubtedly increases the calculation amount of the system; A sliding mode variable structure model reference adaptive system observer based on saturation function, introducing sliding mode control to replace the original PI control, improving the robustness of the system, but smooth saturation function can not guarantee the convergence of the system state, which is not conducive to the stability of the system; The superspiral algorithm (FSTA) and model reference adaptive system (MRAS) are combined to improve the robustness of the system under the premise of suppressing chattering [22]. However, the traditional superspiral algorithm can not deal with linear growth disturbance effectively.

In order to solve the above problems, this paper combines NFTSM and MRAS, and designs a control strategy combining non-singular fast terminal sliding mode controller and model reference adaptive system observer (NFTSMC-MRASO), which is used to estimate motor speed and rotor position. The method can convert the observed torque value into torque current feedforward compensation to the input end of the current loop, avoid large sliding mode gain, and overcome the chattering problem of the system when the external disturbance is suddenly added. At the same time, the system robustness is greatly improved under the premise of suppressing chattering.

2 Mathematical model of PMSM

Permanent magnet synchronous motor (PMSM) is a nonlinear [23], multi-variable, strong coupling complex system. Ignoring the effects of core saturation, hysteresis loss and eddy current loss, and because the stator inductance of PMSM is $L_d = L_q = L_s$, the dynamic mathematical model of PMSM in the rotating coordinate system is

$$\begin{cases} \frac{\mathrm{d}i_d}{\mathrm{d}t} = -\frac{R}{L_s}i_d + \omega_e i_q + \frac{u_d}{L_s} \\ \frac{\mathrm{d}i_q}{\mathrm{d}t} = -\frac{R}{L_s}i_q - \omega_e i_d - \frac{\phi_f}{L_s}w_e + \frac{u_q}{L_s} \end{cases} \tag{1}$$

Where, i_d, i_q, u_d, u_q, L_d and L_q are the stator current, stator voltage and stator inductance in d-q coordinate system respectively; ω_e, R, and ϕ_f are the electric angular speed, stator resistance and rotor permanent magnet flux, respectively.

For the surface mounted permanent magnet synchronous motor [24], using the vector control method with $i_d = 0$, the equation of motion can be expressed as

$$\begin{cases} J\frac{\mathrm{d}\omega_m}{\mathrm{d}t} = T_e - T_L - B\omega_m \\ T_e = 1.5pi_q\varphi_f \end{cases} \tag{2}$$

Where, T_e, T_L , p and ω_m are respectively electromagnetic torque, load torque, number of poles and mechanical angular velocity.

3 Design of NFTSM-MRASO

3.1 Principle of MRASO

The observer of model reference adaptive system mainly consists of a reference model [21], an adjustable model and an adaptive law. The reference model does not contain the parameters to be estimated, and the adjustable model contains the parameters to be estimated. When the system works, the output of the two models has the same physical meaning. Then according to the output error between the two models, a reasonable adaptive law is designed to update the parameters of the adjustable model, so that the output error between the two models tends to zero when the system reaches the steady state.

The basic structure diagram of MRASO is shown in Figure 1.

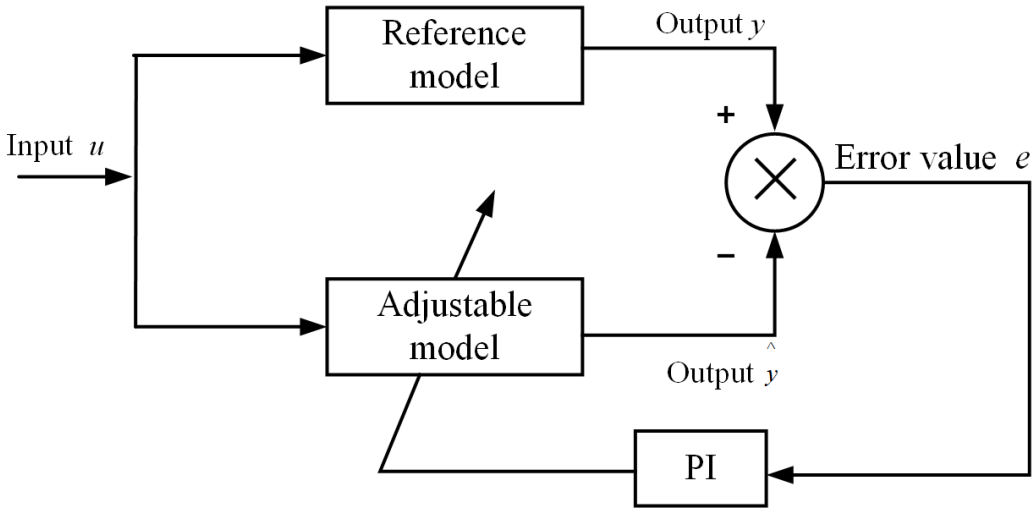

Figure 1: MRASO Structure Diagram

3.2 Design of MRASO

According to the principle of MRASO, reference model and adjustable model are set respectively for dynamic mathematical model.

First, let:

$$\begin{cases} i'_d = i_d + \frac{\varphi_f}{L_s} \\ i'_q = i_q \\ u'_d = u_d + \frac{R\varphi_f}{L_s} \\ u'_q = u_q \end{cases} \tag{3}$$

Set the reference model according to Equation (1), expressed as

$$\begin{bmatrix} \frac{\mathrm{d}i'_d}{\mathrm{d}t} \\ \frac{\mathrm{d}i'_q}{\mathrm{d}t} \end{bmatrix} = \begin{bmatrix} -\frac{R}{L_s} & \omega_e \\ -\omega_e & -\frac{R}{L_s} \end{bmatrix} \begin{bmatrix} i'_d \\ i'_q \end{bmatrix} + \begin{bmatrix} \frac{1}{L_s} & 0 \\ 0 & \frac{1}{L_s} \end{bmatrix} \begin{bmatrix} u'_d \\ u'_q \end{bmatrix} \tag{4}$$

Meanwhile, according to Equation (4), the adjustable model setting is expressed as

$$\begin{bmatrix} \frac{\mathrm{d}\hat{i}'_d}{\mathrm{d}t} \\ \frac{\mathrm{d}\hat{i}'_q}{\mathrm{d}t} \end{bmatrix} = \begin{bmatrix} -\frac{R}{L_s} & \hat{\omega}_e \\ -\hat{\omega}_e & -\frac{R}{L_s} \end{bmatrix} \begin{bmatrix} \hat{i}'_d \\ \hat{i}'_q \end{bmatrix} + \begin{bmatrix} \frac{1}{L_s} & 0 \\ 0 & \frac{1}{L_s} \end{bmatrix} \begin{bmatrix} u'_d \\ u'_q \end{bmatrix} \tag{5}$$

Where, variables with ˆ denote the corresponding estimated value.

By subtracting Equations (4) and (5), we can obtain:

$$\begin{bmatrix} \frac{\mathrm{d}}{\mathrm{d}t}\propto i'_d \\ \frac{\mathrm{d}}{\mathrm{d}t}\propto i'_q \end{bmatrix} = \begin{bmatrix} -\frac{R}{L_s} & \omega_e \\ -\omega_e & -\frac{R}{L_s} \end{bmatrix} \begin{bmatrix} \propto \\ i'_d \\ \propto \\ i'_q \end{bmatrix} + \begin{bmatrix} 0 & \propto \\ & \omega_e \\ \propto & \\ -\omega_e & 0 \end{bmatrix} \begin{bmatrix} \hat{i'_d} \\ \hat{i'_q} \end{bmatrix} \tag{6}$$

Rewrite Equation (6) as

$$\frac{\mathrm{d}}{\mathrm{d}t}\propto i'_s = -F\overset{\propto}{i'_s} - G \tag{7}$$

Where,$F = \begin{bmatrix} -\frac{R}{L_s} & \omega_e \\ -\omega_e & -\frac{R}{L_s} \end{bmatrix}$; $G = \begin{bmatrix} 0 & \propto \\ & \omega_e \\ \propto & \\ -\omega_e & 0 \end{bmatrix} \begin{bmatrix} \hat{i'_d} \\ \hat{i'_q} \end{bmatrix}$.

According to Popov's hyperstability theory [25], for the system to be stable, the estimated speed $\hat{\omega_e}$ and rotor position $\hat{\theta_e}$ should be expressed as

$$\begin{cases} \hat{\omega_e} = \left[K_p + \frac{K_i}{S}\right]\left[i_d\hat{i_q} - i_q\hat{i_d} - \frac{\varphi_f}{L_S}\left(i_q - \hat{i_q}\right)\right] \\ \hat{\theta_e} = \int \hat{\omega_e}\mathrm{d}t \end{cases} \tag{8}$$

3.3 Design of NFTSMC

According to Equation (8), the speed information of the traditional MRASO is obtained through the PI controller. However, in practical engineering applications, PI has the problem of insufficient robustness, so the sliding mode controller is used to replace the original PI controller.

Define sliding mode surface as follows.

$$S = i'_d\hat{i'_q} - i'_q\hat{i'_d} \tag{9}$$

According to the equivalent principle of sliding mode control [26], when the system enters the sliding mode, that is, $S = \dot{S} = 0$, and combined with Equation (3), the following can be obtained:

$$\omega_{eq} = \omega_e + \frac{\frac{2R}{L_S}\left(\hat{i_d}i_q - i_d\hat{i_q}\right) + \left(\frac{R\varphi_f}{L_S^2} - \frac{u_d}{L_S}\right)\left(i_q - \hat{i_q}\right) + \frac{u_q}{L_S}\left(i_d - \hat{i_d}\right)}{\left(\frac{\varphi_f}{L_S}\right)^2 + \frac{\left(i_d + \hat{i_d}\right)\varphi_f}{L_S} + i_q\hat{i_d} + i_d\hat{i_q}} \tag{10}$$

According to Equation (10), when the system enters the sliding mode, that is to say, the currents of the reference model and the adjustable model are equal, that is, $\omega_{eq} = \omega_e$. The estimated speed is expressed as

$$\hat{\omega_e} = \chi sign\left(S\right) \tag{11}$$

Where, χ is the sliding mode gain; $sign(S)$ is the sign function.

As can be seen from Equation (11), the estimated speed contains discontinuous switching functions, which will cause a large number of buffeting phenomena in the system, and it is usually necessary to introduce a first-order low-pass filter for filtering processing, but this increases the complexity of the system.

Therefore, the non-singular fast terminal sliding mode algorithm is used to avoid large sliding mode gain and solve the buffeting problem of the system.

Firstly, it is known from the above that the estimated speed of the motor is $\hat{\omega_e}$, and the actual speed of the motor is ω_e , and the speed error and its rate of change can be obtained:

$$\begin{cases} e = \hat{\omega_e} - \omega_e \\ \dot{e} = \dot{\hat{\omega}_e} - \dot{\omega_e} \end{cases} \tag{12}$$

The expression of Non-singular Fast Terminal Sliding Mode-Controller (NFTSMC) is constructed

$$S\left(x\right) = e + 1/\theta\dot{e}^{p/q} + \gamma\left|e\right|^m \tag{13}$$

Where $S(x)$ is a sliding surface; x is the system state; $\theta > 0$;p and q are both odd numbers greater than 0, and $q < p < 2q$; $m > 0$.

Setting $S = 0$, the rate of change of the velocity error is obtained as

$$\dot{e} = [\theta(-e - \gamma |e|^m)]^{q/p} \tag{14}$$

From the Equation (14), it can be seen that when the system error is moved close to the sliding mode, the error convergence speed depends on the index item. When the system error is close to the balance point, the error convergence speed mainly depends on the linear item, ensuring the global convergence speed, which guarantees the global convergence speed.

Based on the traditional power reaching law, the fast power reaching law is established. This new power reaching law maintains the advantages of the traditional power reaching law, further accelerates the global convergence rate and restrains the system buffeting. Its specific form is given, as follows:

$$\dot{S} = -C |S|^{\alpha} sgn(S) - \varepsilon |e|^{\beta} S \tag{15}$$

Where, $\varepsilon > 0$, $\alpha > 1$ and $\beta \geq 1$. In addition, the definitions of the state variable x_1 and the sliding surface S are still as described above. According to Equation (15), the first term of the improved variable exponential reaching law is the power reaching law, and the second term is the product of an exponential term εS and a power function $|x_1|^{\beta}$ of the state variable. This reaching law is called the variable exponential reaching law, and the reaching advantages of the system are as follows: When the system is far away from the sliding surface, the power term and the variable exponential term work together to speed up the reaching rate and shorten the reaching time. By introducing the state variable, the chattering problem caused by the exponential term can be weakened. When the system is close to the sliding surface, the value of the latter term is very close to 0, so the convergence rate of the system motion state to the sliding surface is mainly determined by the power term, which ensures the global convergence rate.

However, by analyzing the reaching law, it is easy to find that $sgn(S)$ is a discontinuous function, and the reaching law still has a quantity $-C |S|^{\alpha} sgn(S)$ that causes chattering. By decreasing the value of the coefficient C, the chattering of the system can be reduced, but at the same time, it will reduce the speed of the system state variable reaching the sliding mode surface, prolong the stability time of the system, and reduce the control performance of the system. In order to further suppress the chattering problem of the system, the above reaching law is further improved by using a sine saturation function instead of sign function. The saturation function method, also known as the boundary layer method, uses the boundary layer principle to make the system into a continuous system, and the expression of the new sine saturation function is

$$sat(S, \Delta) = \begin{cases} sgn(S) & |S| \geq \Delta \\ sgn(\lambda S) & |S| < \Delta \end{cases} \tag{16}$$

Where, Δ is the thickness of the boundary layer,$\lambda = \pi/2\Delta$. In this way, the switching control is used outside the saturation layer, and the linear control is used inside the saturation layer, which not only ensures the convergence speed, but also reduces the chattering caused by high-frequency switching, and ensures the tracking performance of the motor in medium and low speed occasions.

Then, combined with Equations (2), (13) and (15), the new non-singular fast terminal sliding mode control law is as follows.

$$i_q = \frac{J}{1.5 n_p \varphi_m} \int \left(\frac{\theta q}{p} \dot{e}^{2-p/q} \left(1 + \gamma m |e|^{m-1}\right) + C |S|^{\alpha} sat(S) + \varepsilon |e|^{\beta} S + \frac{T_L}{J} + \frac{B}{J} \omega_m \mathrm{d}t \right) \tag{17}$$

3.4 Stability proof of NFTSMC

The Lyapuov stability condition [27] is used to illustrate it. Now define a Lyapuov function $V(x)$ with first-order partial derivatives as follows

$$V(x) = 1/2 S^2 \tag{18}$$

Taking the derivative yields:

$$\dot{V}(x) = S\dot{S} \tag{19}$$

Equation (13) shows that:

$$\dot{S} = \dot{e} + \frac{p}{\theta q}\dot{e}^{p/q-1}\ddot{e} + \gamma m\left|e\right|^{m-1}\dot{e} = \dot{e} + \frac{p}{\theta q}\dot{e}^{p/q-1}\left(-\frac{3p_n\varphi_m}{2J}\dot{i}_q + \frac{\dot{d}(t)}{J} + \frac{B\dot{\omega}_m}{J}\right) + \gamma m\left|e\right|^{m-1}\dot{e} \tag{20}$$

Put Equation (17) into Equation (15) to obtain

$$\dot{S} = \frac{p}{\theta q}\dot{e}^{p/q-1}\left(-C\left|S\right|^{\alpha} sat(S) - \varepsilon\left|e\right|^{\beta} S\right) \tag{21}$$

Then there is:

$$\dot{V} = S\dot{S} = \frac{p}{\theta q}\dot{e}^{p/q-1}\left(-C\left|S\right|^{\alpha} sat(S)\, S - \varepsilon\left|e\right|^{\beta} S^2\right) \tag{22}$$

Where, since $\theta > 0$, $\alpha > 0$, $C > 0$, $\varepsilon > 0$,$|S| > 0$, $\beta \geq 0$,$|e| > 0$, p and q are positive odd numbers, $\dot{V}(x) \leq 0$, namely, satisfies the sliding mode motion stability condition.

Combined with Equation (2), the designed NFTSMC-MRASO is applied to the sensorless control vector control system of surface-mounted permanent magnet synchronous motor, as shown in Figure 2.

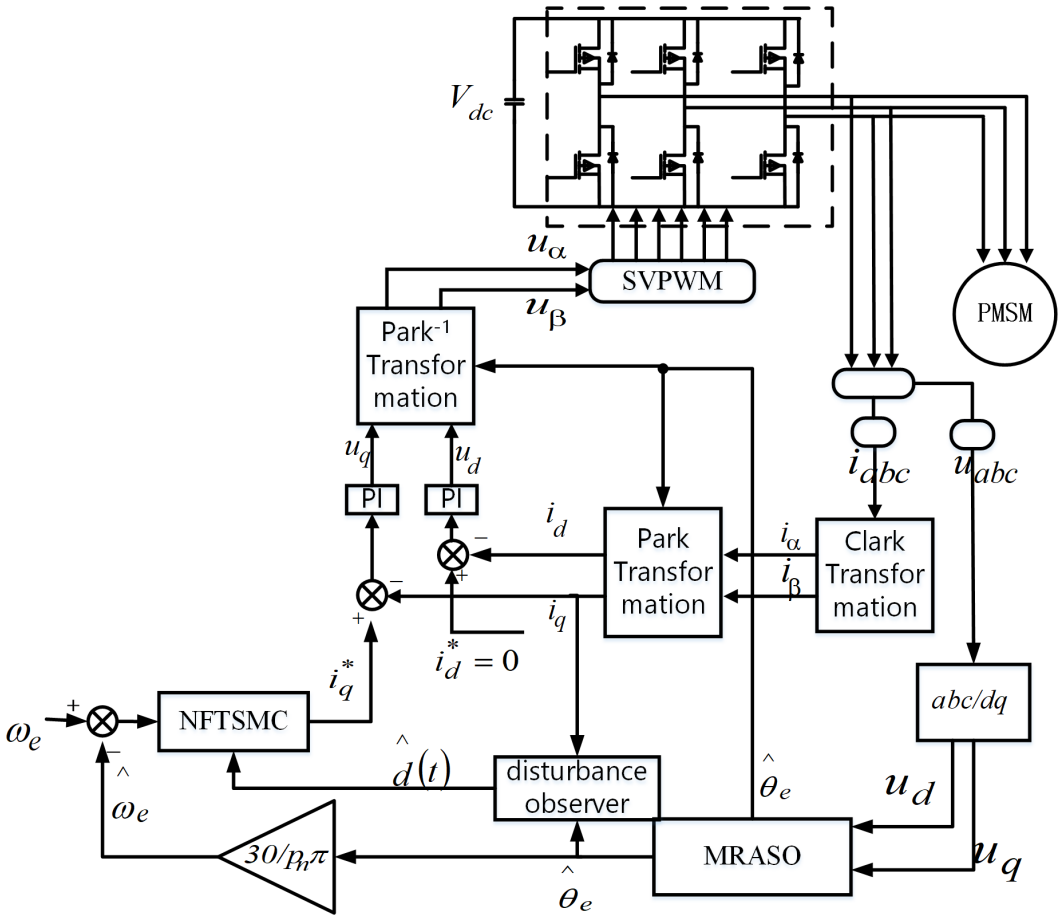

Figure 2: System Control Block Diagram

4 Simulation analysis

In order to prove the effectiveness of the proposed strategy, this paper builds a sensorless control model of SPMSM based on NFTSMC-MRASO through the MATALAB/Simulink simulation platform according to Figure 2, and its motor parameters are shown in Table 1.

Table 1: SPMSM parameters

Parameter names	Parameter values
Number of poles	2
Stator resistance /Ω	2.875
Electronic inductors /mH	8.5
Permanent magnet flux /Wb	0.175
Moment of inertia/(kg.m2)	0.0008
Damping coefficient	0

The controller parameters are PI: $K_p = 15$, $K_i = 3000$; FSTA-SM-MRASO, $\alpha_1 = 3$, $\alpha_2 = 40000$, $k = 5000$; NTSMC-MRASO, $\varepsilon = 400$, $\alpha = 0.54$, $\beta = 3.49$.

Figure 3 shows the simulation figures of the speed response and speed error of four sensorless control strategies: FSTA-SM-MRASO, NTSMC-MRASO, NFTSMC-MRASO, PI-MRASO, when the motor starts with no load at a given speed of 1000 r/min and suddenly increases the load by 3 N.m at 0.2s.

The relative errors of speed of four methods are analyzed respectively. The relative errors of speed of four methods are analyzed respectively. The relative errors of speed of four methods are analyzed respectively.

FSTA-SM-MRASO: $\Delta n_1 = 4.2 - (-4.1) = 8.3r/m$

PI-MRASO: $\Delta n_2 = 3.2 - (-2.5) = 5.7r/m$

NTSMC-MRASO: $\Delta n_3 = 0.75 - (-0.5) = 1.25r/m$

NFTSMC-MRASO: $\Delta n_4 = 0.35 - (0.25) = 0.6r/m$

According to the speed response of Figure 3 (a)-(d), it can be seen that the four sensorless control strategies of PI-MRASO, FSTA-SM-MRASO, NTSMC-MRASO and NFTSMC-MRASO are feasible and effective. The estimated speed of the algorithm can track the actual speed of the motor. Figure 3 (e) can be seen from the speed error. In the motor start and 0.2s load surge phase, the speed estimation of the PI-MRASO control strategy has a large speed error fluctuation, and the estimated speed of the algorithm cannot accurately track the actual speed. When using the FSTA-SM-MRASO control strategy, the speed estimation has good stability in the motor starting and 0.2s load surge stages, but the speed error is the largest among the four methods. Although the NTSMC-MRASO and NFTSMC-MRASO control strategies have good stability and small speed estimation error in the motor starting and 0.2s load surge stages, NFTSMC-MRASO has the smallest speed error, the best dynamic and static performance, and stronger robustness.

Figure 4 shows the simulation figures of the rotor position response of the motor for four different sensorless control strategies, PI-MRASO, FSTA-SM-MRASO, NTSMC-MRASO and NFTSMC-MRASO, when the motor starts with no load at a given speed of 1000 r/min and a sudden load increase of $3\mathrm{N} \cdot \mathrm{m}$ at 0.2s.

From the rotor position response curves of Figure 4 (a) to (d), it can be seen that the four sensorless control strategies of FSTA-SM-MRASO, NTSMC-MRASO, FSTA-SM-MRASO and NFTSMC-MRASO are feasible and effective, and the rotor position of the motor can be tracked by the rotor position of the algorithm.

According to the enlarged figure of rotor position error in Figure 4 (e) and Figure 4 (f), it can be seen that when the PI-MRASO control strategy is adopted, the rotor position estimation error is the largest and has large error fluctuation in the motor starting and load surge stages, and the robustness of the algorithm is poor. When using the FSTA-SM-MRASO control strategy, the rotor position estimation error is improved compared with the PI-MRASO control strategy, and the robustness of the algorithm is also improved. The NTSMC-MRASO and NFTSMC-MRASO control strategies have the smallest rotor position error and good stability in the motor starting and load surge stages. The error comparison diagram of NTSMC-MRASO and NFTSMC-MRASO with Figure 4(g) shows that compared with NTSMC-MRASO, the speed error of NFTSMC-MRASO with linear correction term is smaller, and the dynamic and static performance is better, which can more effectively deal with the disturbance and further suppress the sliding mode chattering. The robustness of the system is

improved.

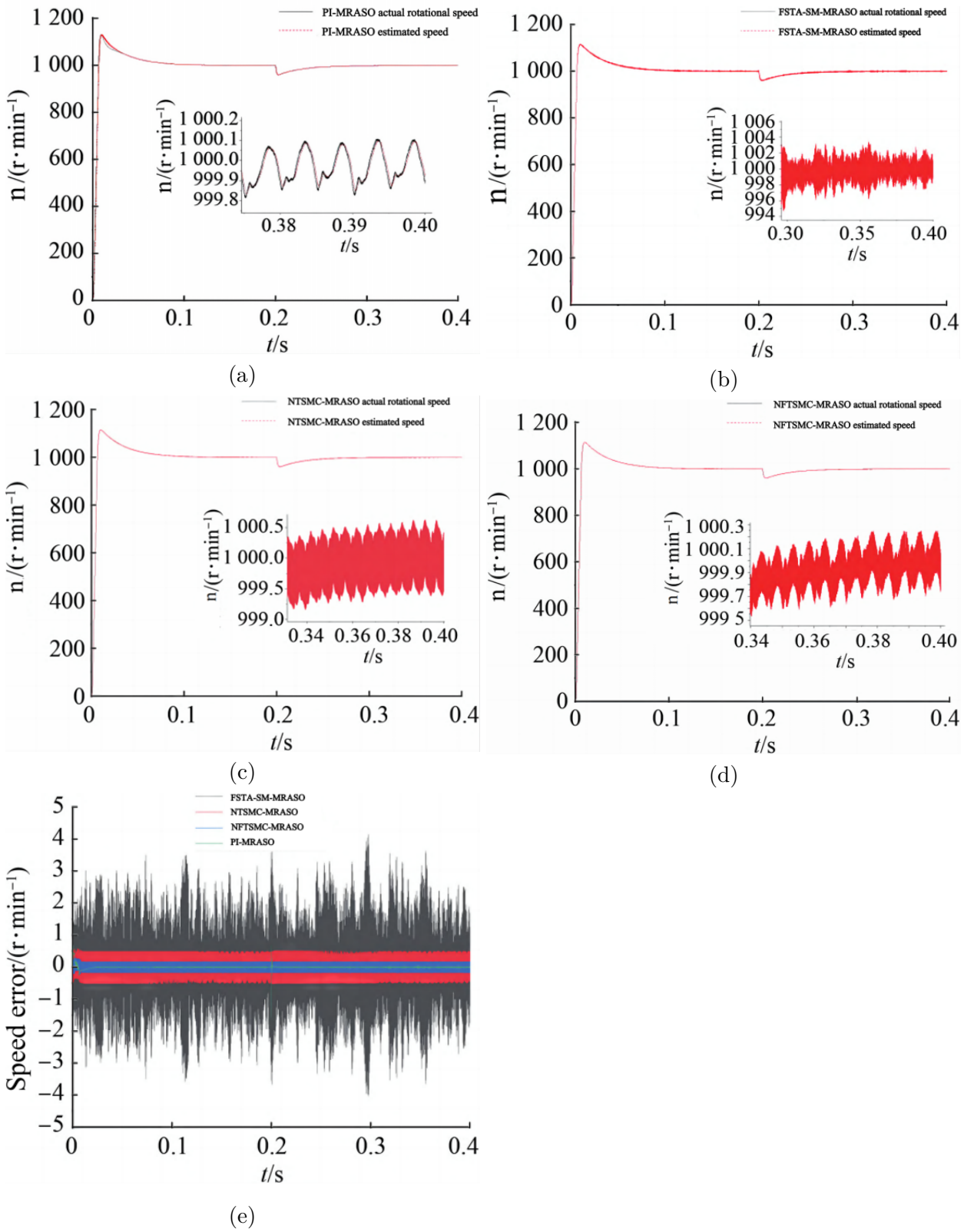

Figure 3: (a) PI-MRASO speed response (b) FSTA-SM-MRASO speed response (c) NTSMC-MRASO speed response (d) NFTSMC-MRASO speed response (e) speed error

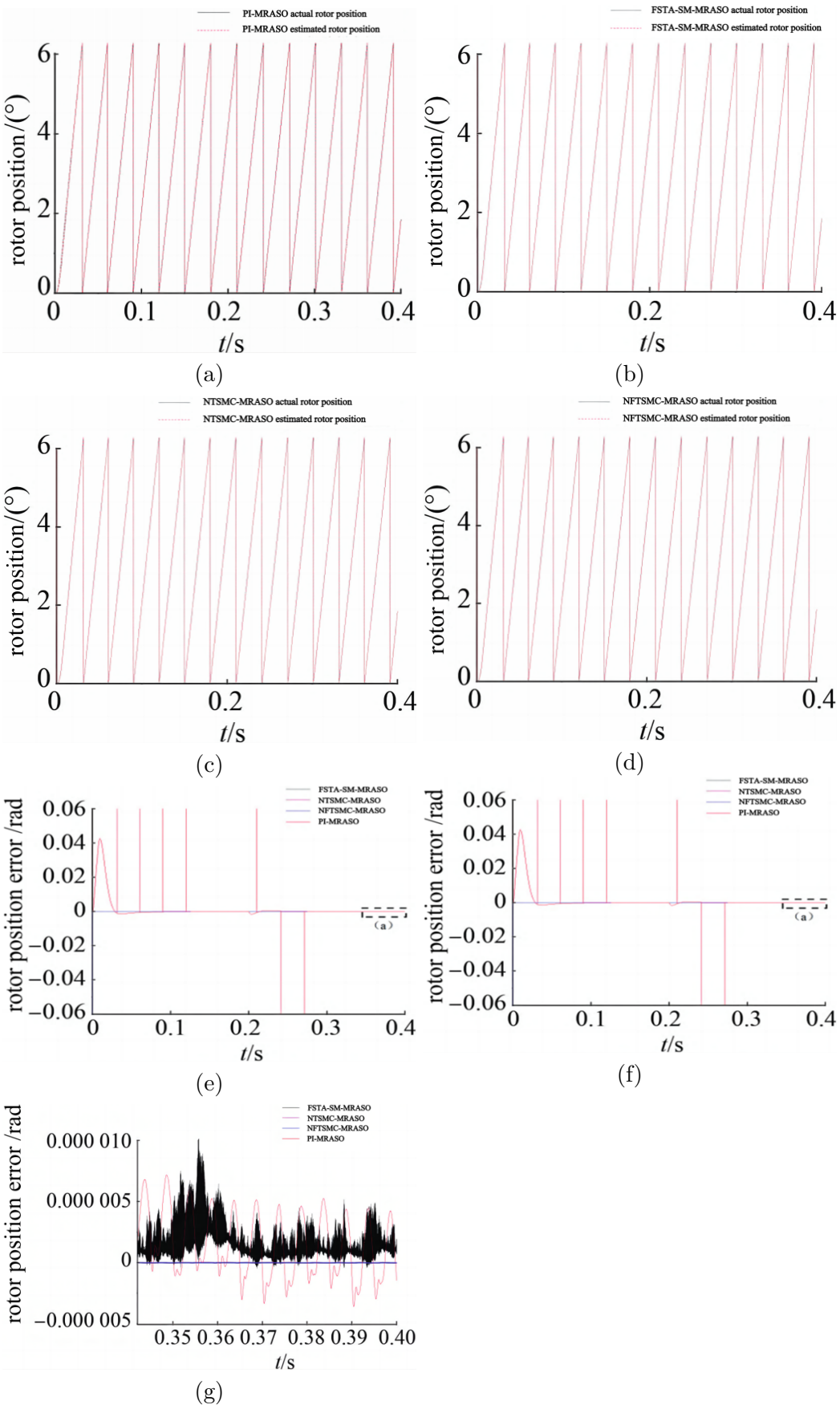

Figure 4: (a) PI-MRASO rotor position response (b) FSTA-SM-MRASO rotor position response (c) NTSMC-MRASO rotor position response (d) NFTSMC-MRASO rotor position response (e) rotor position error (f) enlarged picture of the rotor position error (g) NTSMC-MRASO and NFTSMC-MRASO errors

5 Conclusion

In this paper, a novel sensorless control strategy for PMSM based on NFTSMC-MRASO has been proposed and validated through simulation studies. The main contributions of this work are:

1. The design of a non-singular fast terminal sliding mode controller to suppress chattering and improve system robustness.
2. The integration of NFTSMC with MRASO for accurate speed and rotor position estimation.
3. The use of observed torque value as feedforward compensation to enhance disturbance rejection.

The simulation results demonstrate that the proposed NFTSMC-MRASO outperforms existing methods such as PI-MRASO, FSTA-SM-MRASO, and NTSMC-MRASO in terms of speed response, rotor position tracking, and robustness to sudden load disturbances. The improved accuracy and stability of the proposed approach make it suitable for high-performance PMSM control in various industrial applications, such as automotive, robotics, and aerospace.

However, this study has some limitations, such as the lack of experimental validation and the need for further analysis of parameter selection and optimization. Future work may focus on the following aspects:

1. Experimental implementation of the proposed method on a physical PMSM system.
2. Comparative studies with other state-of-the-art sensorless control techniques.
3. Investigation of adaptive or intelligent parameter tuning methods for enhanced performance.
4. Extension of the proposed approach to other types of motors or multi-motor systems.

In conclusion, the NFTSMC-MRASO provides a promising solution for high-accuracy and robust sensorless control of PMSM. The findings of this research contribute to the advancement of PMSM control technology and have potential implications for various industrial applications.

Conflict of interest

The author declare no conflict of interest.

References

[1] Costantino Citro, Mohammed Al Numay & Pierluigi Siano. (2024). Extensive assessment of virtual synchronous generators in intentional island mode, *International Journal of Electrical Power and Energy Systems*, 109853-.

[2] Marko Č. Bošković, Tomislav B. Šekara, Djordje M. Stojić & Milan R. Rapaić. (2024). Novel tuning rules for PIDC controllers in automatic voltage regulation systems under constraints on robustness and sensitivity to measurement noise, *International Journal of Electrical Power and Energy Systems*, 109791-.

[3] Hossein Mahvash, Seyed Abbas Taher & Josep M. Guerrero. (2024). Mitigation of severe false data injection attacks (FDIAs) in marine current turbine (MCT) type 4 synchronous generator renewable energy using promoted backstepping method, *Renewable Energy*, 120008-.

[4] Badini Sai Shiva, Verma Vimlesh, Tariq Mohd, Urooj Shabana & MihetPopa Lucian. (2022). Performance of a Vector-Controlled PMSM Drive without Using Current Sensors, *Mathematics*, (23), 4623-4623.

[5] Oussama Saadaoui, Amor Khlaief, Moez Abassi, Imen Tlili, Abdelkader Chaari & Mohamed Boussak. (2019). A New Full-Order Sliding Mode Observer Based Rotor Speed and Stator Resistance Estimation for Sensorless Vector Controlled Pmsm Drives, *Asian Journal of Control*, (3), 1318-1327.

[6] Vacis Tatarūnas, Ieva Čiapienė & Agnė Giedraitienė. (2024). Precise Therapy Using the Selective Endogenous Encapsidation for Cellular Delivery Vector System, *Pharmaceutics*, (2).

[7] Stefano Lai, Katarina Kumpf, Philipp Fruhmann, Pier Carlo Ricci, Johannes Bintinger, Annalisa Bonfiglio & Piero Cosseddu. (2024). Optimization of organic field-effect transistor-based mechanical sensors to anisotropic and isotropic deformation detection for wearable and e-skin applications, *Sensors and Actuators A: Physical*, 115101-.

[8] Rezoug Amar, Messah Ayoub, Messaoud Walid Ahmed, Baizid Khelifa & Iqbal Jamshed. (2024). Adaptive-optimal MIMO nonsingular terminal sliding mode control of twin-rotor helicopter system: meta-heuristics and super-twisting based control approach, *Journal of the Brazilian Society of Mechanical Sciences and Engineering*, (3).

[9] Danial Pazoki, Amirhossein Nikoofard & Ali Khaki Sedigh. (2024). Heave attenuation in offshore managed pressure drilling with an integral sliding mode controller, *Applied Ocean Research*, 103932-.

[10] Yury Orlov, Ramón I. Verdés Kairuz & Luis T. Aguilar. (2024). Scaling technique for prescribed-time output feedback stabilization: Autonomous and non-autonomous paradigms and their comparative study, *Journal of the Franklin Institute*, (5), 106642-.

[11] Liu Hsu, José Paulo V.S. Cunha, Ramon R. Costa, Fernando Lizarralde, Eduardo Vieira Leão Nunes, Tiago Roux Oliveira & Alessandro Jacoud Peixoto. (2024). Nyquist criterion for chattering avoidance and global stability in observer-based sliding-mode control with parasitics, *Journal of the Franklin Institute*, (5), 106658-.

[12] Achraf Saadaoui & Mohammed Ouassaid. (2024). Super-twisting sliding mode control approach for battery electric vehicles ultra-fast charger based on Vienna rectifier and three-phase interleaved DC/DC buck converter, *Journal of Energy Storage*, (PB), 110854-.

[13] A S Kolomiytsev, A V Kotosonova, O I Il'in, A V Saenko, A V Shelaev & A V Baryshev. (2024). Novel technology for controlled fabrication of aperture cantilever sensors for scanning near-field optical microscopy, *Micron (Oxford, England : 1993)* , 103610-103610.

[14] GonzálezCely Aura Ximena, Diaz Camilo A R, CallejasCuervo Mauro & BastosFilho Teodiano. (2023). Optical fiber sensors for posture monitoring, ulcer detection and control in a wheelchair: a state-of-the-art, *Disability and rehabilitation: Assistive technology* , 11-18.

[15] Duhancik Michal, Coranic Tomas, Gaspar Stefan & Lipovsky Vladimir. (2022). Sensorless Control Analysis of Electric Motor Drives Based on High-Frequency Signal Injection and Its Simulation Verification, *Actuators*, (11), 317-317.

[16] Hussien Mohamed G., Liu Yi, Xu Wei & Ismail Moustafa Magdi. (2022). Voltage regulation-based sensorless position observer with high-frequency signal injection topology for BDFIGs in ship power microgrid systems, *International Journal of Electrical Power and Energy Systems.*

[17] Khalilnezhad Mohammad Reza & Kopec Dak. (2023). Assessing the macro and micro elements of the Akbarieh World Heritage Garden using participant observer method in a continuous/stop-motion, *Journal of Cultural Heritage Management and Sustainable Development* , (4), 909-926.

[18] Alejandro Clemente, Manuel Montiel, Félix Barreras, Antonio Lozano, Bryan Escachx & Ramon Costa Castelló. (2024). Online estimation of the state of charge and state of health of a vanadium redox flow battery, *Journal of Power Sources*, 234181-.

[19] Pouya Hashemzadeh, Martin Désilets & Marcel Lacroix. (2024). Online state estimation of Li-ion batteries using continuous-discrete nonlinear Kalman filters based on a nonlinear simplified electrochemical model, *Electrochimica Acta*, 143953-.

[20] Krim Saber & Mimouni Mohamed Faouzi. (2023). Design and Xilinx Virtex-field-programmable gate array for hardware in the loop of sensorless second-order sliding mode control and model reference adaptive system-sliding mode observer for direct torque control of induction motor drive, *Proceedings of the Institution of Mechanical Engineers* , (5), 839-869.

[21] Kakodia Sanjay Kumar & Dyanamina Giribabu. (2022). Type-2 Fuzzy Logic controller-based stator current Model reference adaptive system speed observer for a hybrid electric vehicle to improve transient response during limp home mode, *International Journal of Circuit Theory and Applications*, (10), 3426-3442.

[22] Aykut Bıçak & Ayetül Gelen. (2023). Modified Super-Twisting Algorithm-Based Model Reference Adaptive Observer for Sensorless Control of the Interior Permanent-Magnet Synchronous Motor in Electric Vehicles, *Machines*, (9).

[23] Dae Jin Kim & Byungki Kim. (2024). Linear Matrix Inequality-Based Robust Model Predictive Speed Control for a Permanent Magnetic Synchronous Motor with a Disturbance Observer, *Energies*, (4).

[24] (2020). Energy - Electric Power; New Findings from Isfahan University of Technology Describe Advances in Electric Power (Applying a Modified Model Predictive Current Control Method To Improve Surface-mounted Permanent Magnet Synchronous Motor Drives Performance In Transient ...), *Energy Weekly News*, 605-.

[25] Kumar Virendra, Srikanth K.& Grover D. (2023). Darcy–Brinkman analysis of thermo-vibrational convection in gyrotactic swimmers: an overstability theory, *Journal of Thermal Analysis and Calorimetry*, (19), 10189-10201.

[26] (2020). Mathematics; Research from Xi'an Jiaotong University Reveals New Findings on Mathematics (Adaptive Sliding Mode Control Based on Equivalence Principle and Its Application to Chaos Control in a Seven-Dimensional Power System), *Journal of Mathematics*.

[27] Kanika Dhawan, Ramesh Kumar Vats, Ankit Kumar Nain & Anurag Shukla. (2024). Well-posedness and Ulam-Hyers stability of Hilfer fractional differential equations of order (1,2] with nonlocal boundary conditions, *Bulletin des sciences mathématiques*, 103401-.

Journal's webpage: http://univagora.ro/jour/index.php/ijccc/

This journal is a member of, and subscribes to the principles of,
the Committee on Publication Ethics (COPE).
https://publicationethics.org/members/international-journal-computers-communications-and-control

Cite this paper as:

Li,G. (2024). Improved Sliding Mode Model Reference Adaptive System Observer, *International Journal of Computers Communications & Control*, 19(5), 6620, 2024.
https://doi.org/10.15837/ijccc.2024.5.6620